

SCIENTIFIC REPORTS



OPEN

Identifying N⁶-methyladenosine sites using multi-interval nucleotide pair position specificity and support vector machine

Received: 05 January 2017

Accepted: 24 March 2017

Published: 25 April 2017

Pengwei Xing¹, Ran Su², Fei Guo¹ & Leyi Wei¹

N⁶-methyladenosine (m⁶A) refers to methylation of the adenosine nucleotide acid at the nitrogen-6 position. It plays an important role in a series of biological processes, such as splicing events, mRNA exporting, nascent mRNA synthesis, nuclear translocation and translation process. Numerous experiments have been done to successfully characterize m⁶A sites within sequences since high-resolution mapping of m⁶A sites was established. However, as the explosive growth of genomic sequences, using experimental methods to identify m⁶A sites are time-consuming and expensive. Thus, it is highly desirable to develop fast and accurate computational identification methods. In this study, we propose a sequence-based predictor called RAM-NPPS for identifying m⁶A sites within RNA sequences, in which we present a novel feature representation algorithm based on multi-interval nucleotide pair position specificity, and use support vector machine classifier to construct the prediction model. Comparison results show that our proposed method outperforms the state-of-the-art predictors on three benchmark datasets across the three species, indicating the effectiveness and robustness of our method. Moreover, an online webserver implementing the proposed predictor has been established at <http://server.malab.cn/RAM-NPPS/>. It is anticipated to be a useful prediction tool to assist biologists to reveal the mechanisms of m⁶A site functions.

N⁶-methyladenosine (m⁶A) is firstly found in polyadenylated RNA from mammalian cells in the 1970s^{1–4}. Since then, m⁶A is observed in many species, such as *bacteria*, *Homo sapiens*, *Arabidopsis thaliana*, and *Saccharomyces cerevisiae*, etc. It is currently the most hot topic among ~150 RNA-modification types⁵. m⁶A involves many molecular processes, including brain development abnormalities and other diseases⁶, protein translation and localization⁷, and even contributed to obesity⁸. Recent studies have suggested that the regions in 5' untranslated regions (UTRs), around stop codons and in 3' UTRs neighbor stop codons has a number of m⁶A residues^{9,10}, indicating that m⁶A exists high specificity in these regions. Thus, accurate identification of m⁶A sites is the first step to provide in-depth understanding of their biological functions.

In the last few decades, many computational methods have developed for the identification of m⁶A sites. Researchers use the motif discovery algorithm and find that m⁶A peaks has a consensus motif with form of DRACH (where D = A, G or U; R = A or G; H = A, C or U)^{11–15}. These results show m⁶A writers which refer to adenosine methyltransferases including METTL3, METTL14, WTAP, and KIAA1429, and m⁶A erasers which refers to that demethylases including FTO and ALKBH5 may constitute a limited repertoire with predominant and a few less abundant elements¹⁶. At the same time, there are a mass of consensus motifs that are not methylated. To identify methylated m⁶A sites, it is imperative to build a high-resolution data for predicting m⁶A sites. Schwartz *et al.* constructed a single-nucleotide resolution genomic map of m⁶A sites in the *Saccharomyces cerevisiae* species¹³. Using this high resolution data, Chen *et al.* proposed a predictor called “iRNA-Methyl”, which formulates RNA sequences by using “pseudo dinucleotide composition” together with three RNA physiochemical properties to make predictions^{17,18}. Jaffrey *et al.* built a single-nucleotide resolution map of m⁶A sites across *Homo sapiens*¹⁴. Zhou and his co-workers developed a mammalian m⁶A site predictor called SRAMP, which proposed three feature encoding algorithms, such as positional binary encoding of nucleotide sequence, the

¹School of Computer Science and Technology, Tianjin University, Tianjin, China. ²School of Software, Tianjin University, Tianjin, China. Correspondence and requests for materials should be addressed to L.W. (email: weileyi@tju.edu.cn)

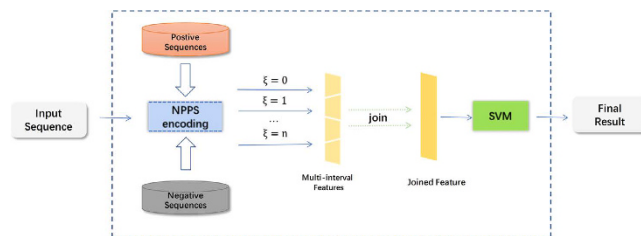


Figure 1. Overall framework of the proposed predictor.

K-nearest neighbor (KNN) encoding, and the nucleotide pair spectrum encoding¹⁹. More recently, Chen *et al.* proposed a support vector machine-based method to predict m⁶A sites in *Arabidopsis thaliana*²⁰. In some studies, well-established ensemble classifiers are proved to outperform single classifiers^{21–23}. Based on this, Chen *et al.* thus proposed a m⁶A predictor by constructing an ensemble classifier based on support vector machine to successfully improve the predictive performance²⁴.

Although many computational efforts have been done in the prediction of m⁶A sites, existing methods are still far from being accurate. The major difficulty is that feature representation algorithms are not informative enough to capture insight differences between true m⁶A sites and non-m⁶A sites²⁵, thus resulting in the low discriminatory ability of feature representations. In this study, we propose a novel feature representation algorithm, in which we sufficiently capture both the global and local information based on multi-interval nucleotide pair position specificity, and successfully convert RNA sequences into high-quality feature representations. Using the proposed feature representations and support vector machine (SVM), we propose a sequence-based predictor called RAM-NPPS for identifying m⁶A sites, where “R” stands for RNA, “A” stands for N⁶-adenosine, “M” stands for methylation, and “NPPS” stands for nucleotide pair position specificity. Comprehensive comparison results on three benchmark datasets across three species show that our proposed RAM-NPPS performs remarkably better than the state-of-the-art predictors. For academic convenience, we establish an online webserver implementing the proposed predictor at <http://server.malab.cn/RAM-NPPS/>.

Materials and Methods

Datasets. As indicated in many previous studies, datasets are fundamentally important to build a robust and accurate prediction model^{26,27}. In this study, we employed three benchmark datasets across three species to comprehensively evaluate the performance of the proposed predictor. The details of the three datasets are described as follows.

Saccharomyces cerevisiae dataset. This dataset is originally proposed by Chen *et al.*²⁸. The dataset contains 1,307 positive sequences with m⁶A sites and 1,307 negative sequences with non-m⁶A sites. It is worth noting that the negative samples are randomly collected from 33,280 sequences with non-m⁶A sites. All sequences in the dataset are 51-nt long (25-nt on each side of the m⁶A/non-m⁶A sites) with the sequence similarity less than 85%.

Homo sapiens dataset. This dataset, downloaded from Zhou’s work¹⁹, recompiles the recently published single-nucleotide resolution maps of mammalian m⁶A sites¹⁴. The dataset contains 8,366 positive samples and the equal number of negative samples. The negative samples are selected from 65,345 negative samples randomly. All sequences in this dataset are 51-nt long as well.

Arabidopsis thaliana dataset. This benchmark dataset is downloaded from Chen’s study²⁰. The dataset contains 394 positive samples and the same number of negative samples. The sequences in this dataset share less than 60% sequence similarity.

For academic convenience, we provide all the three datasets mentioned above in our webserver. They are freely available to be downloaded from the following website: <http://server.malab.cn/RAM-NPPS/data.jsp>.

Framework of the proposed predictor. Figure 1 illustrates the overall framework of the RAM-NPPS method for m⁶A site prediction. The prediction process of the proposed RAM-NPPS predictor is described as follows. Firstly, input sequences are encoded by the proposed NPPS (nucleotide pair position specificity) feature representation algorithm to obtain the meaningful feature vectors. Then, the resulting feature vectors with different parameter (ξ) values are joined together into one. Finally, the joined ones are fed into the SVM classifier to make predictions.

Feature encoding algorithm. For convenience of discussion, the dataset can be denoted as,

$$S = S^+ \cup S^- \quad (1)$$

where S is the entire dataset; S^+ is the set of all positive samples, i.e., all RNA sequences containing m⁶A sites; S^- is the set of all negative samples, i.e., all RNA sequences containing nonk-m⁶A sites.

For a given RNA sequence, it can be encoded with the following formula:

$$P = P^+ - P^- \quad (2)$$

where P^+ is formulated as:

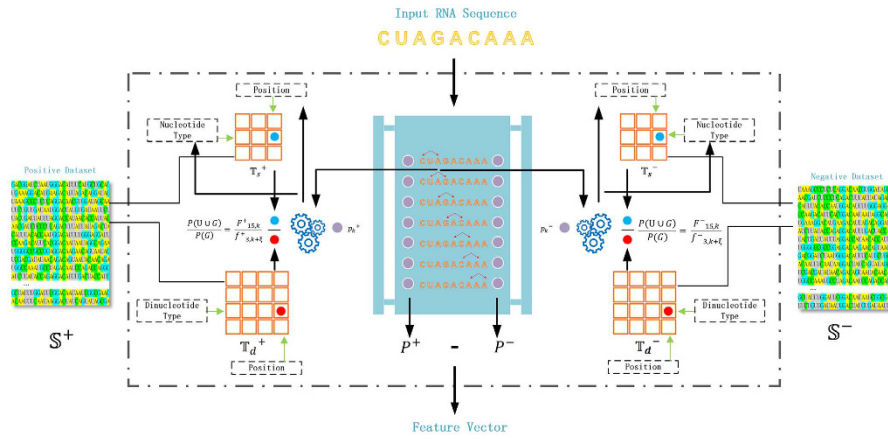


Figure 2. Schematic workflow of the proposed feature encoding scheme.

$$P^+ = p_1^+ p_2^+ \dots p_k^+ \dots p_{l-1}^+ p_l^+ \tag{3}$$

where p_k represents the k -th nucleotide, l is the length of the sequence.

To calculate p_k^+ , let us define two matrices T_s^+ and T_d^+ :

$$T_s^+ = \begin{bmatrix} f_{1,1}^+ & f_{1,2}^+ & \dots & f_{1,l}^+ \\ f_{2,1}^+ & f_{2,2}^+ & \dots & f_{2,l}^+ \\ f_{3,1}^+ & f_{3,2}^+ & \dots & f_{3,l}^+ \\ f_{4,1}^+ & f_{4,2}^+ & \dots & f_{4,l}^+ \end{bmatrix} \tag{4}$$

where rows represent $\{A, C, G, U\}$, respectively; column represents the length of the sequence. The element $f_{1,1}^+$ represents the single nucleotide occurrence probability of the 'A' nucleotide in all positive sequences (samples) at the 1st position of the sequence for example.

$$T_d^+ = \begin{bmatrix} F_{1,1}^+ & F_{1,2}^+ & \dots & F_{1,l}^+ \\ F_{2,1}^+ & F_{2,2}^+ & \dots & F_{2,l}^+ \\ \vdots & \vdots & \ddots & \vdots \\ F_{16,1}^+ & F_{16,2}^+ & \dots & F_{16,l}^+ \end{bmatrix} \tag{5}$$

where rows represent $\{A C G U\} \times \{A C G U\}$, respectively; column represents the length of the RNA sequence; the element $F_{1,2}^+$ represents the occurrence probability of the nucleotide pair 'AC' in all positive samples at the position of 2-nd and $(2 + \xi)$ -th nucleotide of the RNA sequence, where ξ is the interval of the two nucleotides in a pair. It is worth noting that $\xi = 0$ denotes the continuous dinucleotide.

Assuming that the dinucleotide between the k -th nucleotide and $(k + \xi)$ -th nucleotide is 'CG', p_k^+ can be computed the following formula by using the conditional probability formula $p(A|B) = \frac{P(A \cap B)}{P(B)}$,

$$p_k^+ = \frac{P(C \cap G)}{P(G)} = \frac{F_{7,k}^+}{f_{3,k+\xi}^+} \tag{6}$$

where 7 is the index of 'CG' in the $\{A C G U\} \times \{A C G U\}$, and 3 is the index of 'G' in the $\{A C G U\}$.

Accordingly, we obtained P^+ from S^+ . Similarly, we obtained P^- from S^- . Finally, the RNA sequence is successfully converted into the feature vector P by formula (2).

Figure 2 shows the NPPS feature representation process. Firstly, we compute nucleotide position specificity information by counting the occurrence frequency of different nucleotide types at different positions for the positive dataset S^+ and the negative sequence set S^- , respectively. Then, the information is stored in matrices T_s^+ , T_d^+ , T_s^- , and T_d^- . T_s^+ stores single nucleotide position specificity information of the positive sequences and T_d^+ stores nucleotide pair position specificity information of the positive sequences, T_s^- and T_d^- are for negative sequences. When it comes to an input sequence, we can get P^+ and P^- of the input sequence according to the four matrices above. Finally, we successfully encode the input sequence into a feature vector by the subtraction of P^+ and P^- .

In the above process, we can obtain the local sequential information by setting the parameter ξ and getting multi-interval nucleotide pair position information within the sequence. This makes our features reflect relevance of different interval nucleotides. Moreover, by counting frequency of nucleotide position in entire positive dataset and negative dataset, we can get the global information between positive and negative samples.

ξ	Dimension	Sn (%)	Sp (%)	Acc (%)	MCC
0	50	77.35	77.66	77.51	0.5501
1	49	75.75	79.65	77.70	0.5544
2	48	75.29	78.50	76.89	0.5382
3	47	76.82	76.82	76.82	0.5363
4	46	75.67	77.58	76.63	0.5326
5	45	78.12	77.58	77.85	0.5570
6	44	76.82	77.74	77.28	0.5455

Table 1. Results of the proposed features by varying the parameter ξ .

Support Vector Machine (SVM). Support Vector Machine (SVM) is a supervised machine learning method based on statistical theory. Due to its high efficacy for classification task, SVM has been widely applied into bioinformatics^{29–35}. In brief, the algorithm of SVM is to transform sample data with different classes into a high-dimension feature space, and then learn an optimal decision boundary or hyper plane for the data from different classes using kernel functions.

In this study, the LibSVM package (<http://www.csie.ntu.edu.tw/~cjlin/libsvm/>) is employed, which is an implementation of SVM. Radial Basis Function (RBF) is set as the kernel function of SVM. Moreover, there are two parameters (penalty constant C and width) in the SVM algorithm. To build a SVM model with high-level performance, the two parameters are optimized by using the grid search approach based on F-score, which considers both precision and recall of the test to evaluate the two parameters.

Evaluation Metrics. In binary predictors, four metrics are usually used to measure the predictive performance, including sensitivity (Sn), specificity (Sp), Accuracy (Acc), and the Mathew's correlation coefficient (MCC), respectively. In this study, the four metrics are employed to evaluate the performance of m⁶A predictors (binary predictor) as well. They are formulated as:

$$Sn = \frac{TP}{TP + FN} \times 100\% \quad (7)$$

$$Sp = \frac{TN}{TN + FP} \times 100\% \quad (8)$$

$$Acc = \frac{TP + TN}{TP + FN + TN + FP} \times 100\% \quad (9)$$

$$MCC = \frac{TP \times TN - FP \times FN}{\sqrt{(TP + FN) + (TN + FP) + (TP + FP) + (TN + FN)}} \quad (10)$$

where TP, TN, FP and FN is the number of true positive, true negative, false positive, and false negative, respectively. In current study, TP represents the total number of the RNA fragment sequences centered with true m⁶A sites that are predicted as m⁶A sequences correctly; TN represents the total number of the RNA fragment sequences centered with non-m⁶A sites that are predicted as non-m⁶A sequences correctly; FP represents the number of those non-m⁶A sequences that are recognized as m⁶A sequences while FN represents the number of those m⁶A sequences that are recognized as non-m⁶A sequences.

Evaluation Methods. In this study, we employ the *k*-fold cross-validation method to evaluate the performance of m⁶A predictors. In *k*-fold cross-validation, a dataset is randomly partitioned into *k* subsets. Of the *k* subsets, a single subset is retained as the validation data for testing the model, and the remaining *k* – 1 subsets are used as training data. The cross-validation process is then repeated *k* times (the folds), with each of the *k* subsets used exactly once as the validation data. The *k* results from the folds then can be averaged (or otherwise combined) to produce a final performance estimation. 10-fold cross-validation is commonly used.

Results and Discussion

Impact of the parameter ξ . In the proposed NPPS feature algorithm, there is a parameter ξ that describes the interval of the nucleotide pairs. Varying the ξ value generates various features, thereby impacting the predictive performance. To investigate the effect of the parameter ξ , we discuss the performance of models based on features over different values of ξ . Theoretically speaking, the maximum value of parameter ξ is the length of the shortest sequence in the dataset minus one. However, when the parameter ξ is larger than 7, the model built on the features is time-consuming. To simplify the problem, we focus only on the range of ξ from 0 to 6.

Table 1 lists the results evaluated with 10-fold cross-validation by the SVM classifier on the *Saccharomyces cerevisiae* dataset. As seen in Table 1, the prediction model has the best performance when $\xi = 5$, achieving the highest Acc of 77.85% and the MCC of 0.5570. This indicates that when the interval between two nucleotides is equal to 5, the correlation information sufficiently reflects the inner differences between true m⁶A sites and non-m⁶A sites.

Features	Sn (%)	Sp (%)	Acc (%)
NPPS features ($\xi = 5$)	78.12	77.58	77.85
Joined NPPS features	79.04	80.80	79.92
Joined NPPS features using MRMD	76.36	79.42	77.89
Joined NPPS features using RFE	67.18	74.50	70.84
Joined NPPS features using FSDI	67.69	75.38	71.54

Table 2. Predictive results of different features.

Classifiers	Sn (%)	Sp (%)	Acc (%)	MCC
Random Forest	75.67	75.98	75.82	0.5165
SVM	79.04	80.80	79.92	0.5984

Table 3. Performance comparison of different classifiers.

Predictors	Sn (%)	Sp (%)	Acc (%)	MCC	Optimized parameters
RAM-NPPS	78.42	80.87	79.65	0.59	$C = 2048, \gamma = 0.0001220703125$
M6A-HPCS	77.35	67.41	72.38	0.45	$C = 8, \gamma = 0.0625$

Table 4. Comparison of identifying m⁶A sites between different methods on *Saccharomyces cerevisiae* dataset.

Impact of different features. In this section, we did a further feature optimization to join 7 different individual interval features above into 329-dimension feature vector. We tested it on the *Saccharomyces cerevisiae* dataset and compared its performance with that of single interval NPPS features in the same environment. The results are listed in Table 2. As shown in Table 2, by joining all the 7 individual NPPS features, the performance is significantly improved from 77.85% to 79.92% for the Acc. This demonstrates that the correlation information of different intervals is complement to the improved predictive performance. However, simply joining features together easily generates redundant information that probably impacts the predictive performance. To validate whether there is redundant information in the joined features, we further applied three well-established feature reduction algorithms: MRMD (Maximal Relevance and Maximal Distance)³⁶, RFE (Recursive Feature Elimination)³⁷, and FSDI (Feature Selection based on Discernibility and Independence of a feature)³⁸, to remove the redundant features from the joined NPPS features, respectively. Their results are presented in Table 2 as well. It can be seen from Table 2 that using feature reduction techniques does not improve the performance, even decreasing the performance significantly. This observation indicates the following three aspects: (1) there is very few redundant information in the joined NPPS features; (2) some important features/information are removed by using the feature reduction techniques; (3) this further confirms that the NPPS features based on different intervals contain the key correlation information that contributes together to the performance improvement.

Comparisons with different classifiers. To verify the effectiveness of the SVM algorithm, we tested and compared the SVM algorithm with the Random Forest (RF) algorithm. The reason to choose the RF for comparison purpose is that the RF is a powerful classification algorithm, having competitive performance in several bioinformatics fields, such as DNA-binding protein prediction³⁹, methylation site prediction⁴⁰, detection of tubule boundaries⁴¹ and phosphorylation site prediction⁴², etc. To fairly compare the performances of SVM and RF, we performed the two algorithms under the same conditions, such as using the same joined NPPS features for modeling, and employing the same dataset for the performance evaluation. The comparison results evaluated with 10-fold cross validation are summarized in Table 3. As shown in Table 3, the SVM exhibits significantly better performance than the RF in terms of all four metrics. To be specific, the Sn, Sp, Acc, and MCC of the SVM are 79.04%, 80.80%, 79.92%, and 0.598, respectively, which are 3.37%, 4.82%, 4.10%, and 8.19% higher than that of the RF (75.67% for Sn, 75.98% for Sp, 75.82% for Acc, and 0.5165 for MCC). This indicates that the SVM algorithm is more effective than the RF algorithm for accurately identifying true m⁶A sites from non-m⁶A sites.

Comparisons with the state-of-the-art predictors. To verify the performance of the proposed predictor, we performed and compared our predictor with state-of-the-art predictors on three benchmark datasets: the *Saccharomyces cerevisiae*, *Homo sapiens*, and *Arabidopsis thaliana* datasets, respectively. It should point out that the *Homo sapiens* dataset uses single interval NPPS feature for same time-consuming reason.

For the *Saccharomyces cerevisiae* dataset, we compared our predictor with the M6A-HPCS method⁴³. It is worth noting that M6A-HPCS is currently the best-performing method on the *Saccharomyces cerevisiae* dataset. Thus, it is no need to compare with other methods but M6A-HPCS. Table 4 lists the jackknife results of our predictor and the M6A-HPCS method. As shown in Table 4, our predictor remarkably outperforms the M6A-HPCS method in terms of four metrics (Sn, Sp, Acc, and MCC), leading by 1.07% for Sn, 13.46% for Sp, 7.27% for Acc, and 0.14 for MCC, respectively.

Predictors	Sn (%)	Sp (%)	Acc (%)	MCC	Optimized parameters
RAM-NPPS	87.31	91.62	89.47	0.79	$C = 32, \gamma = 0.125$
Chen's method	68.78	100.00	84.39	0.72	$C = 0.5, \gamma = 0.0078125$

Table 5. Comparison of identifying m⁶A sites between different methods on *Arabidopsis thaliana* dataset.

For the *Arabidopsis thaliana* dataset, we compared our predictor with Chen's method²⁰. As shown in Table 5, the same rigorous jackknife test is used to assess the experiment results. We observed that our predictor obtains better performance than Chen's method on this dataset, which further proves the effectiveness of our proposed predictor.

For the *Homo sapiens* dataset, we evaluated our predictor with the same 5-fold cross-validation test like the SRAMP predictor did¹⁹. We compared our predictor with the SRAMP predictor in terms of the AUROC and AUPRC. Our predictor obtained the AUROC of 0.748 and the AUPRC of 0.733, which is competitive with the SRAMP method with the AUROC of 0.797 and the AUPRC of 0.312.

In general, our predictor exhibits relatively high-level performance on three datasets cross three species. This indicates that our predictor is effective and robust for the identification of m⁶A sites cross different species.

Conclusions

In this study, we present a novel feature encoding algorithm with multi-interval nucleotide pair position specificity, which captures not only the single RNA sequence local correlation information of multi-interval nucleotide pairs, but also the global position information, specially the global information of diversity between positive and negative samples. We test the redundant information of feature representations with the MRMD approach, optimize the SVM classifier via grid parameter searching based on F-score, and build a sequence-based predictor called RAM-NPPS for m⁶A site identification. Comparative studies on three benchmark datasets across three types of species indicate that our method is superior to the state-of-the-art methods. We establish a webserver at <http://server.malab.cn/RAM-NPPS/>, where users can submit uncharacterized RNA sequences and we can help to identify potential m⁶A sites within the submitted RNA sequences. In particular, the online predictor provides m⁶A site identification specific for three species: *Saccharomyces cerevisiae*, *Homo sapiens*, and *Arabidopsis thaliana*. It is expected that the online webserver can be a very useful tool for m⁶A site-based research. Moreover, we expect that our proposed feature representation algorithm based on multi-interval nucleotide pair position specificity can be further applied to other protein function prediction fields.

References

- Adams, J. M. & Cory, S. Modified nucleosides and bizarre 5'-termini in mouse myeloma mRNA. *Nature* **255**, 28–33 (1975).
- Desrosiers, R., Friderici, K. & Rottman, F. Identification of methylated nucleosides in messenger RNA from Novikoff hepatoma cells. *Proceedings of the National Academy of Sciences* **71**, 3971–3975 (1974).
- Furuichi, Y. *et al.* Methylated, blocked 5' termini in HeLa cell mRNA. *Proceedings of the National Academy of Sciences* **72**, 1904–1908 (1975).
- Wei, C.-M., Gershowitz, A. & Moss, B. Methylated nucleotides block 5' terminus of HeLa cell messenger RNA. *Cell* **4**, 379–386 (1975).
- Cantara, W. A. *et al.* The RNA Modification Database, RNAMDB: 2011 update. *Nucleic acids research* **39**, D195–201, doi: 10.1093/nar/gkq1028 (2011).
- Meyer, K. D. *et al.* Comprehensive analysis of mRNA methylation reveals enrichment in 3' UTRs and near stop codons. *Cell* **149**, 1635–1646, doi: 10.1016/j.cell.2012.05.003 (2012).
- Meyer, K. D. & Jaffrey, S. R. The dynamic epitranscriptome: N6-methyladenosine and gene expression control. *Nature reviews. Molecular cell biology* **15**, 313–326, doi: 10.1038/nrm3785 (2014).
- Nilsen, T. W. Molecular biology. Internal mRNA methylation finally finds functions. *Science* **343**, 1207–1208, doi: 10.1126/science.1249340 (2014).
- Batista, P. J. *et al.* m⁶A RNA modification controls cell fate transition in mammalian embryonic stem cells. *Cell stem cell* **15**, 707–719 (2014).
- Chen, T. *et al.* m⁶A RNA methylation is regulated by microRNAs and promotes reprogramming to pluripotency. *Cell Stem Cell* **16**, 338 (2015).
- Dominissini, D. *et al.* Topology of the human and mouse m⁶A RNA methylomes revealed by m⁶A-seq. *Nature* **485**, 201–206 (2012).
- Meyer, K. D. *et al.* Comprehensive analysis of mRNA methylation reveals enrichment in 3' UTRs and near stop codons. *Cell* **149**, 1635–1646 (2012).
- Schwartz, S. *et al.* High-resolution mapping reveals a conserved, widespread, dynamic mRNA methylation program in yeast meiosis. *Cell* **155**, 1409–1421 (2013).
- Linder, B. *et al.* Single-nucleotide-resolution mapping of m⁶A and m⁶Am throughout the transcriptome. *Nature methods* **12**, 767–772 (2015).
- Chen, K. *et al.* High-Resolution N6-Methyladenosine (m⁶A) Map Using Photo-Crosslinking-Assisted m⁶A Sequencing. *Angewandte Chemie International Edition* **54**, 1587–1590 (2015).
- Cao, G., Li, H.-B., Yin, Z. & Flavell, R. A. Recent advances in dynamic m⁶A RNA modification. *Open biology* **6**, 160003 (2016).
- Chen, W., Tran, H., Liang, Z., Lin, H. & Zhang, L. Identification and analysis of the N6-methyladenosine in the *Saccharomyces cerevisiae* transcriptome. *Scientific reports* **5** (2015).
- Liu, B. *et al.* Pse-in-One: a web server for generating various modes of pseudo components of DNA, RNA, and protein sequences. *Nucleic Acids Research* **43**, W65–W71 (2015).
- Zhou, Y., Zeng, P., Li, Y.-H., Zhang, Z. & Cui, Q. SRAMP: prediction of mammalian N6-methyladenosine (m⁶A) sites based on sequence-derived features. *Nucleic acids research* **44**, e91–e91 (2016).
- Chen, W., Feng, P., Ding, H. & Lin, H. Identifying N6-methyladenosine sites in the *Arabidopsis thaliana* transcriptome. *Molecular Genetics and Genomics* **291**, 2225–2229 (2016).
- Lin, C. *et al.* LibD3C: Ensemble Classifiers with a Clustering and Dynamic Selection Strategy. *Neurocomputing* **123**, 424–435 (2014).
- Zou, Q. *et al.* Improving tRNAscan-SE annotation results via ensemble classifiers. *Molecular Informatics* **34**, 761–770 (2015).

23. Wei, L., Wan, S., Guo, J. & Wong, K. K. A novel hierarchical selective ensemble classifier with bioinformatics application. *Artificial Intelligence in Medicine*, doi: 10.1016/j.artmed.2017.02.005 (2017).
24. Chen, W., Xing, P. & Zou, Q. Detecting N⁶-methyladenosine sites from RNA transcriptomes using ensemble Support Vector Machines. *Scientific Reports* **7** (2017).
25. Liu, B., Liu, F., Fang, L., Wang, X. & Chou, K.-C. repRNA: a web server for generating various feature vectors of RNA sequences. *Molecular Genetics and Genomics* **291**, 473–481 (2016).
26. Wei, L., Tang, J. & Zou, Q. SkipCPP: An Improved and Promising Method for Predicting Cell-Penetrating Peptides by Adaptive k-skip-n-gram Features. *BMC Genomics* (2017).
27. Wei, L. *et al.* Improved prediction of protein–protein interactions using novel negative samples, features, and an ensemble classifier. *Artificial Intelligence in Medicine*, doi: 10.1016/j.artmed.2017.03.001 (2017).
28. Chen, W., Feng, P., Ding, H., Lin, H. & Chou, K.-C. iRNA-methyl: identifying N⁶-methyladenosine sites using pseudo nucleotide composition. *Analytical biochemistry* **490**, 26–33 (2015).
29. Lin, H., Liang, Z. Y., Tang, H. & Chen, W. Identifying sigma70 promoters with novel pseudo nucleotide composition. *IEEE/ACM transactions on computational biology and bioinformatics*, doi: 10.1109/TCBB.2017.2666141 (2017).
30. Zhang, C. J. *et al.* iOri-Human: identify human origin of replication by incorporating dinucleotide physicochemical properties into pseudo nucleotide composition. *Oncotarget* **7**, 69783–69793, doi: 10.18632/oncotarget.11975 (2016).
31. Yang, H. *et al.* Identification of Secretory Proteins in Mycobacterium tuberculosis Using Pseudo Amino Acid Composition. *BioMed research international* **2016**, 5413903, doi: 10.1155/2016/5413903 (2016).
32. Tang, H., Chen, W. & Lin, H. Identification of immunoglobulins using Chou's pseudo amino acid composition with feature selection technique. *Molecular bioSystems* **12**, 1269–1275, doi: 10.1039/c5mb00883b (2016).
33. Chen, X. X. *et al.* Identification of Bacterial Cell Wall Lyases via Pseudo Amino Acid Composition. *BioMed research international* **2016**, 1654623, doi: 10.1155/2016/1654623 (2016).
34. Liu, B., Wang, S., Long, R. & Chou, K.-C. iRSpot-EL: identify recombination spots with an ensemble learning approach. *Bioinformatics* **33**, 35–41 (2017).
35. Liu, B. *et al.* Combining evolutionary information extracted from frequency profiles with sequence-based kernels for protein remote homology detection. *Bioinformatics* **30**, 472–479 (2014).
36. Zou, Q., Zeng, J., Cao, L. & Ji, R. A novel features ranking metric with application to scalable visual and bioinformatics data classification. *Neurocomputing* **173**, 346–354 (2016).
37. Liu, B. *et al.* A novel electrocardiogram parameterization algorithm and its application in myocardial infarction detection. *Computers in Biology & Medicine* **61**, 178–184 (2015).
38. Xie, J., Wang, M., Zhou, Y. & Li, J. Coordinating Discernibility and Independence Scores of Variables in a 2D Space for Efficient and Accurate Feature Selection. 116–127 (Springer International Publishing, 2016).
39. Wei, L., Tang, J. & Zou, Q. Local-DPP: An Improved DNA-binding Protein Prediction Method by Exploring Local Evolutionary Information. *Information Sciences* **384**, 135–144 (2017).
40. Wei, L., Xing, P., Shi, G., Ji, Z. & Zou, Q. Fast prediction of methylation sites using sequence-based feature selection technique. *IEEE/ACM Transactions on Computational Biology and Bioinformatics*, doi: 10.1109/TCBB.2017.2670558 (2017).
41. Su, R. *et al.* Detection of tubule boundaries based on circular shortest path and polar-transformation of arbitrary shapes. *Journal of microscopy* **264**, 127–142 (2016).
42. Wei, L., Xing, P., Tang, J. & Zou, Q. PhosPred-RF: a novel sequence-based predictor for phosphorylation sites using sequential information only. *IEEE Transactions on NanoBioscience*, doi: 10.1109/TNB.2017.2661756 (2017).
43. Zhang, M. *et al.* Improving m⁶A sites prediction with heuristic selection of nucleotide physical-chemical properties. *Analytical Biochemistry* (2016).

Acknowledgements

We thank to Prof. Quan Zou for his helpful suggestion. This work was supported by the Natural Science Foundation of China (No. 61402326).

Author Contributions

X.P.W. participated in designing the experiments, drafting the manuscript and performing the statistical analysis. R.S., F.G., and L.Y.W. participated in providing ideas. All authors read and approved the final manuscript.

Additional Information

Competing Interests: The authors declare no competing financial interests.

How to cite this article: Xing, P. *et al.* Identifying N⁶-methyladenosine sites using multi-interval nucleotide pair position specificity and support vector machine. *Sci. Rep.* **7**, 46757; doi: 10.1038/srep46757 (2017).

Publisher's note: Springer Nature remains neutral with regard to jurisdictional claims in published maps and institutional affiliations.



This work is licensed under a Creative Commons Attribution 4.0 International License. The images or other third party material in this article are included in the article's Creative Commons license, unless indicated otherwise in the credit line; if the material is not included under the Creative Commons license, users will need to obtain permission from the license holder to reproduce the material. To view a copy of this license, visit <http://creativecommons.org/licenses/by/4.0/>

© The Author(s) 2017